Submitted to The Physical Review

UCRL-18817
Preprint

cy. 2

THE PROPERTIES OF THE NON-SPECULAR LOW ENERGY ELECTRON DIFFRACTION BEAMS SCATTERED BY THE (100) FACE OF FACE CENTERED CUBIC METAL SINGLE CRYSTALS

RECEIVED
LIBRARY AND
DOCUMENTS SECTION

H. H. Farrell and G. A. Somorjai

March 1969

AEC Contract No. W-7405-eng-48

TWO-WEEK LOAN COPY

This is a Library Circulating Copy
which may be borrowed for two weeks.
For a personal retention copy, call
Tech. Info. Division, Ext. 5545

LAWRENCE RADIATION LABORATORY
UNIVERSITY of CALIFORNIA BERKELEY

UCRL-18817

DISCLAIMER

This document was prepared as an account of work sponsored by the United States Government. While this document is believed to contain correct information, neither the United States Government nor any agency thereof, nor the Regents of the University of California, nor any of their employees, makes any warranty, express or implied, or assumes any legal responsibility for the accuracy, completeness, or usefulness of any information, apparatus, product, or process disclosed, or represents that its use would not infringe privately owned rights. Reference herein to any specific commercial product, process, or service by its trade name, trademark, manufacturer, or otherwise, does not necessarily constitute or imply its endorsement, recommendation, or favoring by the United States Government or any agency thereof, or the Regents of the University of California. The views and opinions of authors expressed herein do not necessarily state or reflect those of the United States Government or any agency thereof or the Regents of the University of California.

The Properties of the Non-Specular Low Energy Electron Diffraction Beams Scattered By the (100) Face of Face Centered Cubic Metal Single Crystals

H. H. Farrell and G. A. Somorjai

Inorganic Materials Research Division, Lawrence Radiation Laboratory,
Department of Chemistry,
University of California, Berkeley, California

Abstract

The intensities of the non-specular low energy electron beams diffracted from the Al(100) and Pd(100) surfaces were measured as a function of electron energy in the range 5-200 eV at room temperature. The experimental results were correlated with $I_{h,k}$-eV curves which were obtained from Ni(100), Cu(100), Ag(100) and Au(100) surfaces. Single and double diffraction conditions were adequate to compute the positions of most of the maxima. The double diffraction condition, $2\vec{K}_z = \vec{G}_z$, appears to be especially important at low electron energies. The intensities and shape of the diffraction peaks are strongly influenced by the atomic potential.

Introduction

Experimental low energy electron diffraction studies of metal surfaces have a long history which begins with the Davisson-Germer[1] experiment in 1927. However, unlike the case of X-ray diffraction, theoretical interpretations of the diffraction feature have been incomplete or only partially satisfactory, particularly in the very low energy (less than approximately (100 eV) region. The relatively large values of atomic scattering cross sections for low energy electron diffraction (LEED) necessitate the consideration of multiple scattering phenomena. Recently, E. G. McRae[2] has developed a formally complete and self-consistent theory of dynamical low energy electron diffraction. In the subsequent months, there have been a large number of theoretical papers[3,4,5,6] and calculations[7,8] published which all point out the importance of multiple scattering in analyzing the intensities of the diffraction spots to obtain information about the arrangement of atoms in the surface. Concurrently there is a great demand for complete and suitable experimental data to compare with computational results.[8] The importance of multiple scattering in low energy electron diffraction has been experimentally verified by the observation of two phenomena, a) surface wave resonance and b) the appearance of "secondary" diffraction peaks in the I_{hk}- eV curves. Surface wave resonance accompanies the emergence of new diffraction beams. Perhaps the most dramatic manifestation of this effect occurs when a defocussed specularly reflected beam is monitored at a voltage where a diffracted beam should emerge from the crystal. An easily detectable minimum occurs in the intensity of the

observed diffraction spot.[9] Perhaps more significant verification has also resulted from the observation of "secondary" or fractional order, Bragg peaks in the specularly reflected electron beam when its intensity is monitored as a function of electron energy [I_{00} vs. eV].[9,10] Much of the emphasis up to this time has been placed on the theoretical interpretation of the characteristics of this specularly reflected electron beam (the (00) beam).

A great deal of information could be obtained on the nature of low energy electron diffraction from the properties of the non-specular electron beams. There is already a wealth of experimental data in the literature on these diffracted beams. It is the purpose of this paper to present new and detailed experimental data on the characteristics of non-specular beams from the (100) face of aluminum and palladium surfaces and to correlate these with existing data on other face centered cubic metal surfaces. We hope that the experimental data given here will be applicable to further the development of realistic theoretical calculations. The interplay between accurate experimental data and theoretical calculations should lead to structural analysis of metal surfaces.

Experimental

A conventional Varian LEED apparatus of the post-acceleration type[11] was employed. The back-diffracted electrons were accelerated onto a phosphor (P4 bluish-white) screen on which the diffraction spots were displayed. The resulting fluorescent intensity was monitored with a telephotometer (Gamma Scientific No. 2000 with fiber optics and a

variable aperture 6′ → 3°) as a function of beam voltage. It should be noted that the intensity vs. voltage (I vs. eV) curves were not normalized to eliminate variations in emission current. In the electron gun, a Phillips cathode[12] was used. This was found to have somewhat poorer resolution characteristics (± 5 eV) than the standard Varian gun. To compensate for this, a third grid was installed between the standard suppressor grid and the screen, and was operated as an auxiliary suppressor grid. All measurements were carried out at 10^{-10}-10^{-9} torr ambient pressures.

Aluminum and palladium samples were prepared from ultra-high purity single crystals.[13] These crystals were X-ray oriented to within 2° of the (100) face and the samples were then spark cut to around 1 mm thickness for the palladium and 3 mm for the aluminum. After polishing and etching, the palladium sample was mounted on tantalum holders. Because of the relatively higher solid solubility of aluminum in tantalum, to prevent contamination the aluminum samples were placed in high purity aluminum boats before mounting on the tantalum holders. On both samples, ion bombardment and subsequent annealing heat treatments were used to obtain an ordered surface with sharp diffraction features. Under the conditions employed, no surface structures were to be expected on aluminum.[14] Extensive ion bombardments (>36 hours) and high temperature anneals (>450°C) were used to insure the absence of the amorphous oxide film that commonly accompanies freshly prepared aluminum surfaces. On palladium, however, there are several frequently observed surface structures that are produced by annealing. As these surface structures tend to change the shape of the I_{hk} vs. eV curves even before a new diffraction pattern

is observable on the screen, we have followed a technique that both we[15] and Park[16] have employed previously to produce a "normal" (100) surface on Pd which exhibits a (1 x 1) diffraction pattern. A very light ion bombardment (2×10^{-5} torr argon at 150 eV for 10 minutes) was employed followed by a short anneal (less than 400°C for 50 minutes) just before performing the measurements.

Results

The intensities of several of the low index diffraction beams as a function of accelerating voltage are shown in Figure 1 for the (100) face of aluminum, and in Figure 2 for the (100) face of palladium. The intensities from the non-specularly reflected beams were measured within a degree of normal incidence (within a degree). As it is impossible to measure the intensity of the specularly reflected beam, (0,0) beam, at normal incidence with a post-acceleration apparatus, these intensities were obtained at an angle of incidence of 3° with respect to the surface normal. It should be noted that the data is presented as obtained in the experiments. That is, there have been no corrections made for the current vs. voltage characteristics of the electron gun (the current increases sharply with increasing beam voltage) nor for contact potential and other errors in the measured accelerating potential or for changes in the background intensity. The measurements were performed at room temperature (25°C). Consequently, above 150 eV, much of the elastically scattered intensity from aluminum is obscured by the Debye-Waller effect[17] and multi-phonon processes[18] which are responsible for most of the background intensity. In Figure 3

we show a schematic diffraction pattern from a (100) surface with the assignments we have used to identify the diffraction spots. The position of the diffraction peaks (the electron energy at which the intensity is at a maximum) from other experiments on (100) faces of several f.c.c. metals previously reported in the literature[14b,16,19,20,21] are tabulated, with the data from this laboratory, in Table I. A more detailed comparison is made for the (1,0) and (1,1) beams from several metals in Figures 4a and 4b. Here, the energy scale has been "normalized" to compensate for variations in the lattice parameter among the metals [I_{hk} vs. $eVd^2\cos^2\theta$]. As was also found for the specularly reflected (00) beams,[15] the peak positions for the different materials seem to fall at the same corrected electron energies when they are plotted on this "normalized" scale. However, the intensities of these peaks vary considerably from material to material, presumably reflecting variations in the characteristics of the atomic potentials. Certain trends have been noted, and will be discussed in more detail below.

Discussion

A. Single and Double Diffraction Conditions

The prominent features of low energy electron diffraction are the result of atomic scattering cross sections that are much larger than those in X-ray diffraction. In X-ray diffraction, the primary beam intensity is much larger than the intensity of the scattered beams. Thus, the probability that an X-ray which is scattered once will be rescattered again is very small. As a consequence, the only important diffraction conditions are the classical Bragg conditions which may be

written as

$$\vec{K}' - \vec{K}^{\circ} = \vec{G} \tag{1}$$

where $\vec{K}^{\circ}$ is the wave vector of the primary beam, $\vec{K}'$ is the wave vector of a diffracted beam, and $\vec{G}$ is a reciprocal lattice vector. Here, inner potential corrections have been neglected. In low energy electron diffraction, where the cross sections are relatively large, the amplitudes of the various diffracted beams can be of the same order of magnitude as the amplitude of the primary (or incident) beam. As a result, there is a significant probability that an electron may be scattered at least twice before leaving the crystal. Thus, the diffracted beams themselves may behave as "primary" beams or sources of electrons for subsequent scattering events. These double scattering events are characterized by diffraction conditions of the form

$$\vec{K}' - \vec{K}'' = \vec{G} \tag{2}$$

Here, the primes refer to two different diffracted beams. Equation (1) is a special case of this equation. The derivation, and implications of Equation (2) have been extensively discussed by E. G. McRae.[2a] It should be noted that because of these probable multiple scattering events, there may be considerable intensity not only where Equation (1) is met, but also at electron energies and scattering angles where Equation (2) is met. It is one of the features of multiple scattering models that, as observed experimentally for low energy electron diffraction, the intensity vs. energy curves may be more complex than predicted by a single scattering model. Thus, within the double diffraction approximation, to predict the

position of maxima in the I vs. eV curves we must find the electron energies at which Equation (2) is met. While double diffraction considerations may be employed to predict the position (i.e. energy or wave length) at which these diffractions are met, higher order multiple scattering events may contribute to the scattering amplitudes at these positions.

In low energy electron diffraction, the wave vectors of the diffracted beams are uniquely defined by the energy of the electron, the lattice periodicity and the experimental geometry. For elastic scattering, we have the constraint that

$$|\vec{K}^{\circ}| = |\vec{K}'| = \frac{2\pi}{\lambda} = 2\pi\,(eV/150.4)^{1/2} \tag{3}$$

where $\vec{K}^{\circ}$ and $\vec{K}'$ are defined above, λ is the wave length of the electron, and eV is its energy in electron volts. Further, the components of wave vectors that are parallel to the surface must obey the two-dimensional diffraction grating formula

$$\vec{K}'_{xy} = \vec{K}^{\circ}_{xy} + \vec{G}_{xy} \tag{4}$$

where $\vec{K}'_{xy}$ and $\vec{K}^{\circ}_{xy}$ are the components of the wave vectors of the diffracted and the incident beams, respectively, which are parallel to the surface plane, and $\vec{G}_{xy}$ is a reciprocal lattice vector also parallel to the surface plane. It may be seen from Equation (4) that Equation (2) is always obeyed for the <u>parallel</u> components of the wave vectors for all electron energies and scattering angles. Therefore, we need only consider under what conditions Equation (2) is met for the components of

the wave vectors that are perpendicular to the surface. Rewriting Equation (2) for the perpendicular components we have

$$\vec{K}_z' - \vec{K}_z'' = \vec{G}_z \tag{5}$$

where K_z' and K_z'' are the components of the wave vectors of two diffracted beams which are perpendicular to the surface plane, and $\vec{G}_z$ is some reciprocal lattice vector which is also perpendicular to the surface. From the constraints of elastic scattering, and the two-dimensional grating formula (Equations 3 and 4) the magnitude of the component of the diffracted beam perpendicular to the surface, $|\vec{K}_z'|$, is uniquely defined as

$$|\vec{K}_z'| = [|\vec{K}^\circ|^2 - |\vec{K}_{xy}'|^2]^{1/2} . \tag{6}$$

The perpendicular component, $\vec{K}_z'$, may have both positive and negative values, corresponding to beams directed into, or out of the crystal.

The advantages of monitoring the intensities of the non-specular beams at <u>normal electron beam incidence</u> are immediately obvious. Under these conditions, all of the diffraction beams with the same indices and the same sign of $\vec{K}_z'$ are degenerate. Consequently, considerably fewer diffraction conditions of the form given in Equation (5) need be considered. For example, in the region between approximately 20 and 40 eV, in addition to the transmitted and the specularly reflected beams, there exist only the first order diffraction beams, four directed into and four scattered out of the crystal. At normal incidence, the four beams in these two sets are degenerate. Therefore, there are only

four unique beams in this energy range at normal incidence, and we need only consider three equations of the form of Equation (5). However, away from normal incidence, there may be ten unique beams in this same energy range, and it may be necessary to consider up to forty-five diffraction conditions. The situation becomes increasingly complex as one goes to higher voltage ranges.

Further simplification results from the use of the (100) surface in these studies. The interplanar distances are identical in the two perpendicular directions $a_x \equiv a_x$. Thus the parallel components of the lattice vector are identical ($\vec{G}_x \equiv \vec{G}_y$).

In Table II we have tabulated the voltages at which Equation (5) is met for the different beams at normal incidence, for scattering from the (100) face of several f.c.c. metals, and in the absence of inner potential corrections. These calculated positions for the intensity maxima may be compared with those observed experimentally. The various observed peaks are tentatively assigned to the different simple and double diffraction mechanisms. The method used to compute the peak positions of the different single and double diffraction beams from the (100) crystal surfaces at normal incidence is described in the Appendix.

B. Difficulties of Assignments Due to Experimental Uncertainties

It should be emphasized that all of these assignments are tentative and have been made on the basis of the best fit between the calculated and the observed peak positions. Two important parameters have been neglected in arriving at these assignments. The first is inner potential, and the second is that due to experimental inaccuracies.

All of the data which were reported from other laboratories were obtained via faraday cup detectors.[19,20,21] This published data was generally accompanied by detailed correlations between the angle at which a diffraction feature was observed and that calculated from the plane grating formula using the experimental beam voltage. It may be seen that in the low eV region (below 50 or 100 eV), as noted by Farnsworth[19] the agreement is quite good. This agreement between data and calculations seems to indicate that small inner potential corrections on the order of 5 eV or less are appropriate in this region. Cursory studies in this laboratory gave similar results for palladium surfaces.

We have observed that in using the commercial display instruments, serious discrepancies may exist between the measured electron energy, and the actual energy of the electrons striking the crystal. This difference increases with increasing beam voltage and is a function of the temperature of the cathode. This discrepancy results in an uncertainty (as much as 5-20 eV) in determining the electron energy at which diffraction peaks appear. Significant shifts of the I_{hk} vs. eV curves may occur along the voltage scale as a result of minor changes in the cathode characteristics. It was not verified if this same effect exists for the instruments used in the previously published data, but the good agreement between the calculated and the observed angles would seem to indicate that at least it could not have been significant in the low electron energy region.

Another possible source of experimental error was small uncertainties in the angle of incidence. It was found that slight deviations from normal incidence resulted in noticeable shifts in peak positions and

changes in peak shape. These variations increased with increasing beam voltage.

All of these effects tend to make the assignments at the higher beam voltages less reliable than those at the lower beam voltages.

In order to discuss the properties of the different non-specular beams separately, and to correlate them to single and double diffraction events it is useful to arbitrarily divide the electron energy range in which they were studied into four ranges; I) 0-20 eV, II) 20-40 eV, III) 40-80 eV and IV) > 80 eV.

C. Beam Voltage Range ~ 0-20 eV

In this region, below the appearance voltage of the first order diffraction beams, only the specularly reflected beam (00-reflection) is directly observable. There are only two elastic scattering phenomena expected in this region. The first is the appearance of a Bragg peak, ($2\ K_z^\circ = G_z$), predicted by both the single (kinematic) and the multiple scattering theories. The second phenomena is the resonance maximum predicted solely by the multiple scattering approach and discussed in detail by McRae.[2a] Just below the beam voltage at which the first order diffraction beams appear for the (100) face of a simple cubic crystal, there should be a maximum in the specularly reflected (00) beam. This should be immediately followed by a resonance minimum in the (00) beam at the emergence voltage of the (10) beam. This resonance minimum has been experimentally observed on LiF[9] and is considered to be one of the experimental verifications of the multiple scattering nature of low energy electrons (in addition to the presence of double diffraction peaks).

In the experimentally observed specularly reflected (00) beam intensities from the (100) faces of aluminum and palladium, only one maximum is observed in this region, at around 10 eV and 15 eV, respectively. These values are slightly higher than those expected for the appearance of the Bragg maxima. It should be noted that the quality of the data is relatively poor in this low voltage region due to the low current levels of the electron gun. A more detailed investigation in this range with constant current electron source and using more sensitive detection techniques would be useful.

D. Beam Voltage Range ~ 20-40 eV

The second region which starts above the appearance voltage of the first order diffraction (10) beams, but ends just below the appearance voltage of the second order diffraction beams is more complex than the first region due to the increase in the number of beams that are present [(00) and (10)]. At the emergence voltage, a diffraction condition of the form $\vec{K}_z^{10} - \vec{K}_z^{10} = \vec{G}_z$, is met, where $\vec{G}_z$ is the perpendicular component of the reciprocal lattice vector with zero magnitude. This, of course, is the condition for surface wave resonance. This intensity maximum which should appear in the (10) beam has not been observed in any of the data reported here, presumably because of experimental limitations. However, Jones[3] has observed high intensity first order diffraction beams at the emergence voltage.

The second phenomena in this region, which should occur at a slightly higher beam voltage, is characterized by a diffraction condition of

the form $K_z^{00} + K_z^{10} = G_z$. If single scattering predominates, this diffraction process would produce an intensity maximum only in the first order, (10), diffraction beam. Multiple scattering considerations indicate that there should be a maximum in the specularly reflected beam as well.

The available experimental data for the first order diffraction beams from aluminum and palladium do not extend into this low voltage range. However, for silver,[20,21] copper[21] and nickel,[19] intensity maxima are reported in the (10) beams within about 1 eV of the respective calculated values for the single scattering process ($K_z^{00} + K_z^{10} = G_z$). No equivalent peak has been reported for gold, but it may have been outside of the range of experimental observation.[20]

The next predicted maximum involves a diffraction condition of the form $2K_z^{10} = G_z$. This is strictly a multiple scattering effect as it formally necessitates at least double diffraction. This region is still outside of the experimentally observed range for palladium, but maxima have been observed for aluminum,[14b] nickel,[19] copper,[21] gold[20] and silver[20,21] within 3 eV of the respective calculated theoretical values. The maxima for nickel is distinct but weak in the curves reported by Park[19a] and appears only as a shoulder in the curves reported by Farnsworth.[19b] This is an example of the sensitivity of peak shape and position to slight variations in the experimental arrangement.

This peak is of particular interest for several reasons. First, it is forbidden in the kinematic limit of diffraction and therefore may be taken as evidence of multiple scattering. Secondly, it is the first of a general class of dominant peaks (ignoring surface wave resonance)

that are characterized by the equation, $2\vec{K}_z = \vec{G}_z$. Here the diffraction interaction involves beams differing primarily in the sign, but not the magnitude of that component of their wave vector (or momentum) that is perpendicular to the surface.

At a slightly higher beam voltage, there is predicted, a 1/2-ordered secondary Bragg maximum in the specularly reflected beam. This effect has been discussed by McRae[4b] and is associated with a diffraction condition of the form $\vec{K}_z^{00} - \vec{K}_z^{10} = 1/2\ \vec{G}_z$. In the first order diffracted beams from the (100) face of Au and Ag,[20,21] and possibly from Ni[19c] and Cu,[21] there appear intensity maxima in this voltage region. It should be noted that all of these maxima appear at uniformly higher voltages than those predicted.

The relative intensity of this maxima generally increases with increasing atomic number. That is, it is not observed on aluminum,[14b] is weak or questionable on nickel[19] and copper[21] but is quite prominent for gold and silver.[20,21] This region for palladium was outside of the range of experimental observation. Regardless of the assignment of this diffraction peak, this trend in intensities is a manifestation of the effect of varying the potential at the scattering centers by varying the atomic number.

There are no further maxima in the first order diffraction beams below the emergence voltage of the (11) diffraction beams. All of the preceding phenomena may contribute to the intensity of the specularly reflected beam in this region. Comparisons with experiment are complicated by the fact that the intensities of the specularly reflected beam can not be obtained at normal incidence. Aluminum shows a rather

featureless hump in this region at $0 \sim 3°$. Palladium shows a gradual increase in intensity throughout the region. More structure is observable on copper[21] where there are two distinct maxima in this region. It is probable that all of the phenomena contribute to the intensity of the (00) beam in this range. Careful angular studies should allow one to distinguish among the various components.

E. Beam Voltage Range ~ 40-80 eV

This is the region between the appearance of the second order diffraction beams (11) and the third order diffraction beams (20). For the (100) face of face centered cubic metals at normal incidence, the appearance of the (11) beams coincides with the second Bragg maxima in the specularly reflected beam. McRae[2a] has concluded that there should be a zero in the reflectivity curve for the h,k beam when the following two conditions are met simultaneously $K_{h,k} = n2\pi/d$ and $K_{h',k'} = 0$. In this case, the first condition corresponds to the Bragg maxima in the (0,0) beam, and the second to the surface wave resonance in the (11) beams. Consequently, at normal incidence, there should be a minima in the specularly reflected beam in this region in the fully elastic multiple scattering model. Such a minima is observed for aluminum, and possibly for copper.[21] Data for gold, silver and nickel were not investigated. No such minima is observed in the specular, (00) beam, for palladium. As all of the data for the specularly reflected beam was taken at non-normal incidence, it is difficult to conclude anything about the magnitude of this effect for these materials. It is possible that the intensity of this diffraction feature becomes more pronounced with decreasing atomic number.

The first diffraction condition that is met after the appearance of the (11) beams is between the (11) beams and the (10) beams and is characterized by a diffraction condition of the form $K_z^{10} + K_z^{11} = G_z$. This may produce observable maxima in either set of beams. No intensity maxima have been reported in this region for the (11) beam, possibly due to the experimental difficulties inherent in investigating a beam this close to its emergence voltage. The (10) beam represents a different case however. Here the experimental data is reliable, and an intensity maxima is definitely observed in this region for both aluminum[14b] and nickel[19] within 2 eV of the calculated values. In addition, there is a definite shoulder for silver[21] just below 40 eV (calculated value 38.6 eV). No maxima have been reported in this region for the (10) beams from gold[20] and copper,[21] but it is possible that they may be present as a shoulder or a very weak peak masked by adjacent phenomena. The data for palladium does not extend into this region.

At higher energies, there are two diffraction conditions that are met almost simultaneously. The first is of the form $2K_z^{11} = G_z$, and, approximately one electron volt higher, there is another of the form $K_z^{00} + K_z^{10} = G_z$. Except perhaps for nickel, there is a uniform absence of significant intensity maxima in the (10) beams in this range (approximately 45-55 eV for Pd(100)). However, for the (11) beams, definite maxima are observed for silver,[20,21] copper[21] and nickel within several electron volts of the positions calculated from $2K_z^{11} = G_z$. Similarly, there appears to be a shoulder in this region for gold. There is a conspicuous absence of any strong maxima in this range in the data from palladium.[16] The curves for aluminum do not extend into this range. This is a region

where intensity maxima in the (10) beams that should be allowed in the kinematic limit are not observed, possibly being suppressed by a multiple scattering event involving the (11) beams.

Proceeding to still higher energies, we encounter strong maxima in the (10) beams diffracted from all of the materials under investigation. All of the positions are within three electron volts of those calculated from the diffraction condition $2K_z^{10} = G_z$ and there are no other diffraction conditions involving this beam within approximately a 10 volt range. These maxima are generally quite strong and represent one of the more notable and consistent correlations between materials made in this study. As these peaks are relatively strong, they tend to dominate a fairly large energy range. As a result, weaker peaks may be obscured making interpretation in adjacent regions somewhat difficult.

On the high energy side of these intensity maxima in the (10) beam there is some indication of a shoulder for several materials, and definite maxima for both gold[20] and silver.[20,21] The higher peaks on silver and gold are within five and three electron volts respectively of the positions calculated for a half order Bragg peak in the specularly reflected beam that would involve a diffraction interaction between the (00) and the (10) beams. However, they are within three and one electron volts, respectively, of the positions calculated for the diffraction condition $K_z^{10} + K_z^{11} = G_z$. There are no corresponding peaks reported in the (11) beams for any of the materials observed in this range.

At slightly lower energies (62.5 eV for palladium) there are definite intensity maxima in the (11) beams for all of the materials investigated in this region. Furthermore, all of these maxima are within one eV

of the positions calculated from the diffraction condition $K_z^{00} + K_z^{11} = G_z$, with the exception of that for silver[21] which is within three eV of the calculated position. These maxima presumably are a manifestation of a diffraction condition that is allowed in the limit of kinematic scattering.

F. Beam Voltage Range > 80 eV

The next diffraction process of interest is the appearance of the (2,0) diffraction beams and approximately 20 eV higher, the (2,1) beams. It becomes excessively tedious to enumerate in detail all of the possible diffraction conditions as the number of possible types of interaction increases rapidly with the number of beams present even at normal incidence. Away from normal incidence, the situation should be considerably more complicated. Furthermore, as the band structure becomes more complex, bands overlap and the interpretation becomes more difficult. Fewer of the diffraction conditions are met "purely", i.e., without any mixing and not all of the allowed conditions will be observed as multiple scattering may become less pronounced. Comparisons with experimental data also become less reliable at higher beam voltages unless extreme care was exercised in obtaining that data. In general, however, the analysis can be carried out in the same manner as above. The results of such an analysis are tabulated in Table II. There are several points of interest. At normal incidence, the appearance of the (2,0) beams coincides exactly with a diffraction condition of the form $2K_z^{11} = G_z$ for the (1,1) beam. Therefore, a diffraction condition of the form $K_z^{11} - K_z^{20} = G_z$ is automatically met. Accordingly, there should be a

resonance minima in the back reflected (1,1) beam intensity.[2a] In fact, no strong maxima are observed or reported for the (1,1) beams in this region for any of the materials under consideration. This may be taken as an indication of the significance of the resonance effect in this region for these materials. It should be noted that there are very weak maxima observed in this general region for the (1,1) beams of several of these materials.[19,20,21] However, on palladium it has been noted that this beam is very sensitive to position and that its appearance is probably due to small deviations from perfectly normal incidence.

As with the n = 2 Bragg peak, there is a similar coincidence for the n = 4 Bragg peak. In fact, it may be shown that all of the even integral order Bragg peaks from the (100) face of fcc materials at $\theta = 0°$ coincide with the appearance of some set of (h,h) beams. Consequently, there should be a resonance minima rather than a Bragg maxima at these voltages in the fully elastic multiple scattering treatment developed by McRae.[2a] On Al, Pd, Pt,[15] and Cu[21], a minimum is observed in the specular reflected beam at the appropriate voltage. However, on all of these materials, a strong maxima is observed approximately 20 eV lower. It is tempting to assign this to a Bragg peak with a reasonable inner potential and say that the resonance minima is not observed. The former may be correct, but the latter is not necessarily so as all the observations were carried out at $\theta = 0°$. McRae[2a] has shown that for slight deviations from normal incidence, the Bragg peak may appear and that its shape structure may still be strongly influenced by the coupling with the surface wave resonance that accompany the emergence of the new diffraction beams.

There is another interesting feature in this region that may be associated with simultaneous diffraction conditions. On aluminum, very strong intensity maxima in the (1,0) beam occurs at approximately 100 eV. There are at least four diffraction conditions which may be met; $2K^{10} = G_z$, $K_z^{10} + K_z^{21} = G_z$, $2K_z^{21} = G_z$ and $K_z^{10} - K_z^{21} = G_z$. On the high energy side of this maxima for aluminum, a definite shoulder is observable. Going to the corresponding region on nickel,[19a,19b] one finds that the relative intensity of the shoulder is comparable to that of the main beam. Continuing to the noble metals, it may be seen that the peak that was so intense for aluminum has essentially vanished, and that the region is dominated by what was the shoulder. It would be interesting to investigate the behavior of the (2,1) beams in this range in order to observe whether or not they manifest the inverse trend in intensities. If so, this would provide an interesting correlation between scattering amplitudes and potentials for the different metals.

Conclusion

The properties of the non-specular low energy electron beams seem to verify the importance of multiple scattering in low energy electron diffraction. This is consistent with earlier observations on the specularly reflected beam.[9] The number of observed diffraction maxima is too large to allow for their assignment solely on the basis of kinematic considerations. The coincidence of observed intensity maxima positions with those calculated on the basis of a double diffraction mechanism would seem to substantiate the validity of the double diffraction approach[4b] in predicting possible peak positions [though not their intensities]

The double diffraction condition, $2K_z' = \vec{G}_z$ appears to be particularly dominant in the electron energy just above the appearance energy of the beam under consideration. There also appears to be a general tendency for diffraction conditions with relatively small magnitudes of $\vec{G}$ to dominate. As most atomic potentials would favor forward scattering this is physically reasonable.[22]

Assuming that the preceding assignments are at least partially correct, inner potential corrections appear to be considerably less than 10 eV and probably less than 5 eV in the very low energy range. This would be in agreement with the earlier angular studies by Farnsworth.[21] Finally, it may be seen that the atomic potential plays a significant role in determining peak shape and intensity.

Acknowledgement. This work was performed under the auspices of the United States Atomic Energy Commission.

References

1. C. Davisson and L. H. Germer, Proc. Nat. Acad., 14, 619 (1928).

2a. E. G. McRae, J. Chem. Phys., 45(9), 3258 (1966).

2b. E. G. McRae, Surf. Sci., 8, 14 (1967).

3. D. S. Boudreaux and V. Heine, Surf. Sci, 8, 426 (1967).

4a. E. G. McRae, Surf. Sci., 11, 479 (1968).

4b. E. G. McRae, Surf. Sci., 11, 492 (1968).

5a. K. Kambe, Z. Naturforsch., 22A, 322 (1967).

5b. K. Kambe, Z. Naturforsch., 22A, 422 (1967).

6. K. Kambe, Z. Naturforsch., 23A, 1280 (1968).

7. G. Gafner, Calculation of Back-Reflected Leed Intensities Using a Plane Wave Multiple Scattering Mechanism in the Structure and Chemistry of Solid Surfaces, G. A. Somorjai, ed., Proceedings of the Fourth International Materials Symposium, Berkeley, 1968.

8. P. M. Marcus and D. W. Jepsen, Phys. Rev. Letters, 20, 925 (1968).

9. E. G. McRae, Surf. Sci., 7, 41 (1967).

10a. P. J. Estrup and J. Anderson, Surf. Sci., 8, 101 (1967).

10b. N. J. Taylor, Surf. Sci., 4, 161 (1966).

11. Varian, Low Energy Electron Diffraction System, Model No. 981-0000, 611 Hansen Way, Palo Alto, California, U.S.A.

12. Philips Metalonics, Impregnated Cathode, Type B, 88 S. Columbus Avenue, Mt. Vernon, New York.

13. Materials Research Corporation, Post Office Box 14, Redwood City, California.

14a. F. Jona, J. Phys. Chem. Solids, 28, 2155 (1967).

14b. S. M. Bedair, F. Hofmann and H. P. Smith, J. Appl. Phys., 39(8), 4026 (1968).

15. R. M. Goodman, H. H. Farrell and G. A. Somorjai, J. Chem. Phys., 49(2), 692 (1968).

16. R. L. Park and H. H. Madden, Jr., Surf. Sci., 11(2), 188 (1968).

17. R. M. Goodman, H. H. Farrell and G. A. Somorjai, J. Chem. Phys., 48(3), 1046 (1968).

18. E. R. Jones, J. T. McKinney and M. B. Webb, Phys. Rev., 151(2), 476 (1966).

19a. R. L. Park, J. Appl. Phys., 37(1), 295 (1966).

19b. H. E. Farnsworth, et al., J. Appl. Phys., 29(8), 1150 (1958).

19c. M. Onchi and H. E. Farnsworth, Surf. Sci., 11(2), 203 (1968).

20. H. E. Farnsworth, Phys. Rev., 43, 900 (1933).

21. H. E. Farnsworth, Phys. Rev., 40, 684 (1932).

22. This generalization, of course, is not meant to preclude oscillatory behavior in the form factors with increasing values of $|\vec{G}|$.

Appendix

The wave vector of the incident electron beam may be expressed in a Cartesian Coordinate System as

$$\vec{K}^{\circ} = \vec{K}_x + \vec{K}_y + \vec{K}_z \quad . \tag{7}$$

Defining θ as the angle of incidence with respect to the surface normal and φ as the azimuthal angle we have

$$|\vec{K}_x| = |\vec{K}^{\circ}| \sin\theta \sin\varphi \tag{8a}$$

$$|\vec{K}_y| = |\vec{K}^{\circ}| \sin\theta \cos\varphi \tag{8b}$$

$$|\vec{K}_z| = |\vec{K}^{\circ}| \cos\theta \quad . \tag{8c}$$

Using Equation (4) and Equations (8a) and (8b), the x and y components of the wave vector characterizing a diffracted beam can be written as

$$|\vec{K}_x'| = |\vec{K}^{\circ}| \sin\theta \sin\varphi + |\vec{G}_x'| \tag{9a}$$

$$|\vec{K}_y'| = |\vec{K}^{\circ}| \sin\theta \cos\varphi + |\vec{G}_y'| \quad . \tag{9b}$$

Substituting Equations (9a) and (9b) into Equation (6), we obtain

$$|\vec{K}_z'| = \pm \{ |\vec{K}^{\circ}|^2 - (|\vec{K}^{\circ}| \sin\theta \sin\varphi + |\vec{G}_x'|)^2 - (|\vec{K}^{\circ}| \sin\theta \cos\varphi + |\vec{G}_y'|)^2 \}^{1/2} \tag{10}$$

for the component of the diffracted wave vector that is perpendicular to the surface. At normal incidence, $\theta = 0°$ Equation (10) becomes

$$|\vec{K}'|_z = \pm \{ |\vec{K}^{\circ}|^2 - |\vec{G}_x'|^2 - |\vec{G}_y'|^2 \}^{1/2} \tag{11}$$

Substituting Equation (11) into the diffraction equation, Equation (5), we have

$$\pm \{|\vec{K}^\circ|^2 - |\vec{G}_x'|^2 - |\vec{G}_y'|^2\}^{1/2} \mp \{|\vec{K}^\circ|^2 - |\vec{G}_x''|^2 - |\vec{G}_y''|^2\}^{1/2} = |\vec{G}_z| \quad (12)$$

where the appropriate signs are taken for the situation under consideration. Noting that

$$|\vec{K}^\circ| = 2\pi \{eV/150.4\}^{1/2} \; ; \quad |\vec{G}_x| = 2\pi\, h/a_x \; ; \quad |\vec{G}_y| = 2\pi\, k/a_y$$

and $|\vec{G}_z| = 2\pi\, n_z/a_z$, Equation (12) may be written as

$$\pm \{\frac{eV}{150.4} - (\frac{h'}{a_x})^2 - (\frac{k'}{a_y})^2\}^{1/2} \mp \{\frac{eV}{150.4} - (\frac{h''}{a_x})^2 - (\frac{k''}{a_y})^2\}^{1/2} = \frac{n_z}{a_z} \quad (13)$$

where $\vec{a}_x$ and $\vec{a}_y$ are the primitive translations in the two dimensional lattice net parallel to the surface, and $|\vec{a}_z|$ is the distance between planes that are parallel to the surface. For the (100) face of face centered cubic materials, $|\vec{a}_x| = |\vec{a}_y| = \frac{a_o}{\sqrt{2}}$ and $|\vec{a}_z| = \frac{a_o}{2}$ where a_o is the characteristic dimension of the x-ray unit cell (e.g., 4.04 A° for aluminum). Therefore, for the metals reported on here, Equation (13) becomes

$$\pm \{\frac{eV}{150.4} - \frac{2}{a_o^2}[(h')^2 + (k')^2]\}^{1/2} \mp \{\frac{eV}{150.4} - \frac{2}{a_o^2}[(h'')^2 + (k'')^2]\}^{1/2} = \frac{2n_z}{a_o} \quad (14)$$

This equation may be solved analytically, numerically or graphically to determine at what electron energy (in eV) the n_z diffraction condition between the (h', k') beam and the (h'', k'') beam is met.

Table I

Experimentally observed positions (in electron volts) of intensity maxima in non-specularly diffracted beams for the (100) faces of several face centered cubic crystals at normal incidence.

First Order (01) Diffraction Beams					
Al[a] (100) (eV)	Pd[a] (100) (eV)	Ag[b] (100) (eV)	Au[c] (100) (eV)	Cu[d] (100) (eV)	Ni[e] (100) (eV)
59	57	20	27.5	26.5	29
72	78	27	32.0	37.3	35
110	98	34.0	55.0	69.7	47
135	120	56.0	64.0	87.0	55
170	141	62.0	117.0	127.5	62
180	173	115.0		146.0	70
29[f]	203	168.3		220.0	92
40[f]		175.5		243.0	132
					145
					187

Table I continued

Second Order (11) Diffraction Beams

Al[a] (100) (eV)	Pd[a] (100) (eV)	Ag[b] (100) (eV)	Au[c] (100) (eV)	Cu[d] (100) (eV)	Ni[h] (100) (eV)
60	81	46.1	58.0	60.3	65
88	106	55	101.5	72.5	78
118	150	75.7	136.0	115.5	100
150	202	93.5	247.0	128.5	120
190	235	141.0		191.5	153
237	625[g]	229.5		210.5	190
		335.5		296.5	
				310.5	

Table I continued

Third Order (02) Diffraction Beams

Al[a] (100) (eV)	Pd[a] (100) (eV)	Ag[b] (100) (eV)	Au[c] (100) (eV)	Cu[d] (100) (eV)
130	174	77.5	70.0	99.0
168	215	112.5	78.5	111.0
200		158.5	120.0	138.0
		173.5	163.0	154.5
		250.5	256.0	203.0
				215.0
				320.0

Fifth Order (22) Diffraction Beams

Ag[b] (100) (eV)	Au[c] (100) (eV)	Cu[d] (100) (eV)
152.5	171.0	200.5
206.5	191.0	260.5
280.5	303.0	277.0

Table I continued

(a) This laboratory average of several runs.

(b) Reference 20 and Reference 21.

(c) Reference 20.

(d) Reference 21.

(e) References 19a, 19b and 19c - averaged.

(f) Reference 14b.

(g) Reference 16.

(h) Reference 19a.

Calculated and Observed Positions of Intensity Maxima
From the (100) Face of Several Face Centered Cubic Metals

Table IIa
First Order (01) Diffraction Beams

h_x	k_y	h'_x	k'_y	n_z	Al(100) Calc. (eV)	Al(100) Obs.[a] (eV)	Pd(100) Calc. (eV)	Pd(100) Obs.[a] (eV)	Ag(100) Calc. (eV)	Ag(100) Obs.[b] (eV)	Au(100) Calc. (eV)	Au(100) Obs.[c] (eV)	Cu(100) Calc. (eV)	Cu(100) Obs.[d] (eV)	Ni(100) Calc. (eV)	Ni(100) Obs.[e] (eV)
0	1	0	1	0	18.4		20.0		18.1		18.1		23.0		24.3	
0	0	0	1	1	21		23		21	20	21		26	26.5	28	29
0	1	0	1	1	28	29[f]	30		28	27	28	27.5	35	37.3	37	35
										34		32				47
0	1	1	1	1	39	40[f]	43		39		39		49		52	55
0	0	0	1	2	47		51		46		46		58		61	62
0	1	0	1	2	56	59	60	57	54	56	54	55	69	69.7	73	70
0	1	1	1	2	66		71		64	62	64	64	81		86	
						72		78						87		92
0	1	0	2	1	76		82		74		74		95		101	
0	1	0	2	2	88		96		87		87		110		116	
								98								
0	0	0	1	3	94		101		91		91		115		121	

Table IIa continued

h_x	k_y	h'_x	k'_y	n_z	Al(100) Calc. (eV)	Al(100) Obs.[a] (eV)	Pd(100) Calc. (eV)	Pd(100) Obs.[a] (eV)	Ag(100) Calc. (eV)	Ag(100) Obs.[b] (eV)	Au(100) Calc. (eV)	Au(100) Obs.[c] (eV)	Cu(100) Calc. (eV)	Cu(100) Obs.[d] (eV)	Ni(100) Calc. (eV)	Ni(100) Obs.[e] (eV)
0	1	1	2	1												
0	1	1	2	2	102		110		100		100		127	127.5	133	132
0	1	0	1	3												
0	1	1	1	3	112	110	121	120	109		109		138		146	145
						115				115		117		146		
0	1	0	2	3	132	135	143	141	128		128		165		173	
0	1	2	1	3	143		155		140		140		179		188	187

(a) This laboratory average of several runs.

(b) Reference 20 and Reference 21.

(c) Reference 20.

(d) Reference 21.

(e) References 19a, 19b and 19c - averaged.

(f) Reference 14b.

(g) Reference 16.

(h) Reference 19a.

Table IIb

Second Order (11) Diffraction Beams

h_x k_y h'_x k'_y n_z	Al(100) Calc. (eV)	Al(100) Obs.[a] (eV)	Pd(100) Calc. (eV)	Pd(100) Obs.[a] (eV)	Ag(100) Calc. (eV)	Ag(100) Obs.[b] (eV)	Au(100) Calc. (eV)	Au(100) Obs.[c] (eV)	Cu(100) Calc. (eV)	Cu(100) Obs.[d] (eV)	Ni(100) Calc. (eV)	Ni(100) Obs.[h] (eV)
1 1 1 1 0 0 0 1 1 ±1	37		40		36		36		46		48	
0 1 1 1 1	39		43		39		39		49		52	
1 1 1 1 1	46		50		46	46.1	46		58	60.3	61	65
0 0 1 1 2	58		63	62.5[g]	57	55	57	58.0	72	72.5	76	78
0 1 1 1 2	66		71		64		64		81		86	
1 1 1 1 2 1 1 0 2 ±1	74		80	81	72	75.7	72		92		97	100
1 1 1 2 -1 1 1 0 2 2 1 1 2 1 +1	94	88	103	106	92	93.5	92		118	115.5	125	120

Table IIb continued

h_x	k_y	h'_x	k'_y	n_z	Al(100) Calc. (eV)	Al(100) Obs.[a] (eV)	Pd(100) Calc. (eV)	Pd(100) Obs.[a] (eV)	Ag(100) Calc. (eV)	Ag(100) Obs.[b] (eV)	Au(100) Calc. (eV)	Au(100) Obs.[c] (eV)	Cu(100) Calc. (eV)	Cu(100) Obs.[d] (eV)	Ni(100) Calc. (eV)	Ni(100) Obs.[h] (eV)
0	0	1	1	3	104		112		101		101	101.5	128	128.5	135	
1	1	1	2	2	107		116		105		105		133		140	
0	1	1	1	3	112		121		109		109		138		146	
1	1	1	1	3	121	118	130		118		118		150		157	153
1	1	0	2	3	141		152	150	137	141	137	136.0	180		188	190

(a) This laboratory average of several runs.

(b) Reference 20 and Reference 21.

(c) Reference 20.

(d) Reference 21.

(e) Reference 19a, 19b and 19c - averaged.

(f) Reference 14b.

(g) Reference 16.

(h) Reference 19a.

Table IIc

Third Order (02) Diffraction Beams

h_x	k_y	h'_x	k'_y	n_z	Al(100) Calc. (eV)	Al(100) Obs.[a] (eV)	Ag(100) Calc. (eV)	Ag(100) Obs.[b] (eV)	Au(100) Calc. (eV)	Au(100) Obs.[c] (eV)	Cu(100) Calc. (eV)	Cu(100) Obs.[d] (eV)
0	2	0	2	0	73		72		72	70.0	92	
1	1	0	2	±1								
0	1	0	2	-1	76		74		74		95	
								77		78.5		99
0	2	0	2	1	82		81		81		104	
0	0	0	2	-1								
0	0	0	2	2								
0	1	0	2	2	88		87		87		110	111.0
1	1	0	2	2	95		93		93		118	
1	2	0	2	1								
0	2	0	2	2	111		109	112	109		138	138

Table IIc continued

h_x	k_y	h'_x	k'_y	n_z	Al(100) Calc. (eV)	Al(100) Obs.[a] (eV)	Ag(100) Calc. (eV)	Ag(100) Obs.[b] (eV)	Au(100) Calc. (eV)	Au(100) Obs.[c] (eV)	Cu(100) Calc. (eV)	Cu(100) Obs.[d] (eV)
1	2	0	2	2	121		118		118		150	
0	0	0	2	3	125		121		121	120	155	154.5
0	1	0	2	3	132	130	128		128		165	
1	1	0	2	3	141		137		137		176	

(a) This laboratory average of several runs.

(b) Reference 20 and Reference 21.

(c) Reference 20.

(d) Reference 21.

(e) Reference 19a, 19b and 19c - averaged.

(f) Reference 14b.

(g) Reference 16.

(h) Reference 19a.

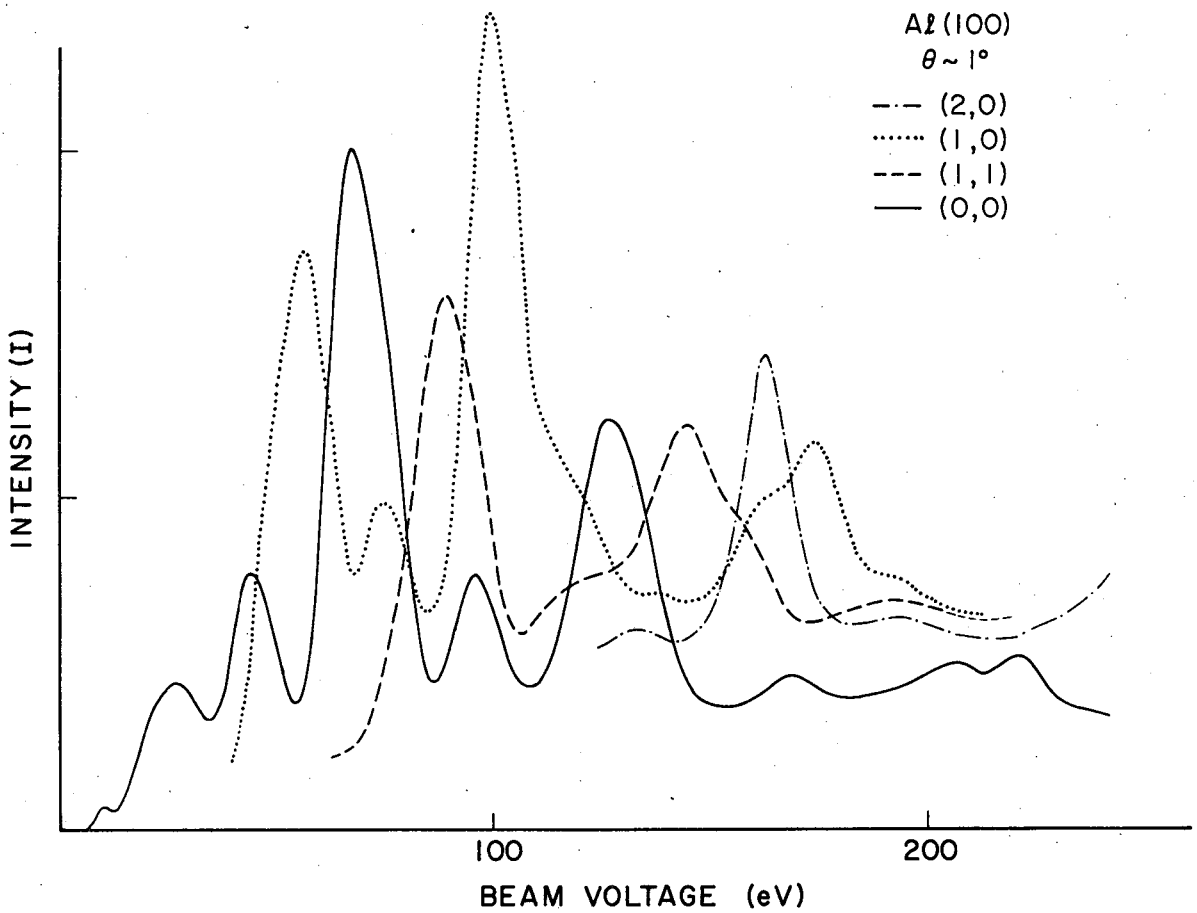

XBL 687-1451

Figure 1. The intensities of several diffraction beams from the Al(100) surface as a function of electron energy.

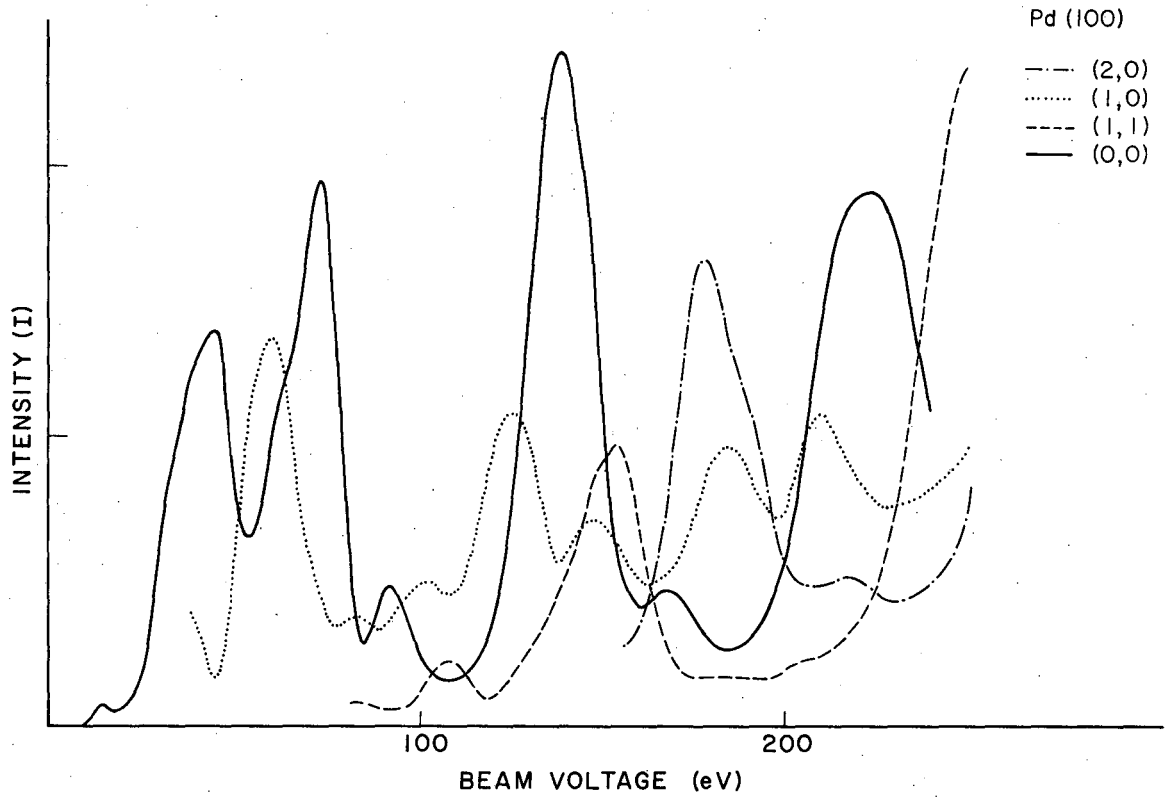

Figure 2. The intensities of several diffraction beams from the Pd(100) surface as a function of electron energy.

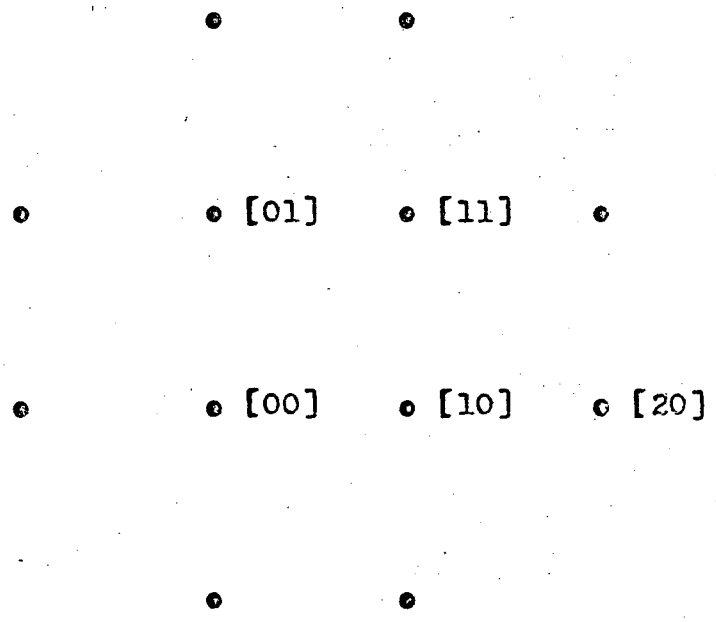

Figure 3. Schematic diffraction pattern from the (100) surface of f.c.c. solids indicating the assignments used to identify the diffraction beams.

Figures 4a and 4b. The intensities of the a) (10) and b (11) diffraction beams as a function of normalized electron energy for the (100) face of aluminum, copper, nickel, palladium, silver and gold.

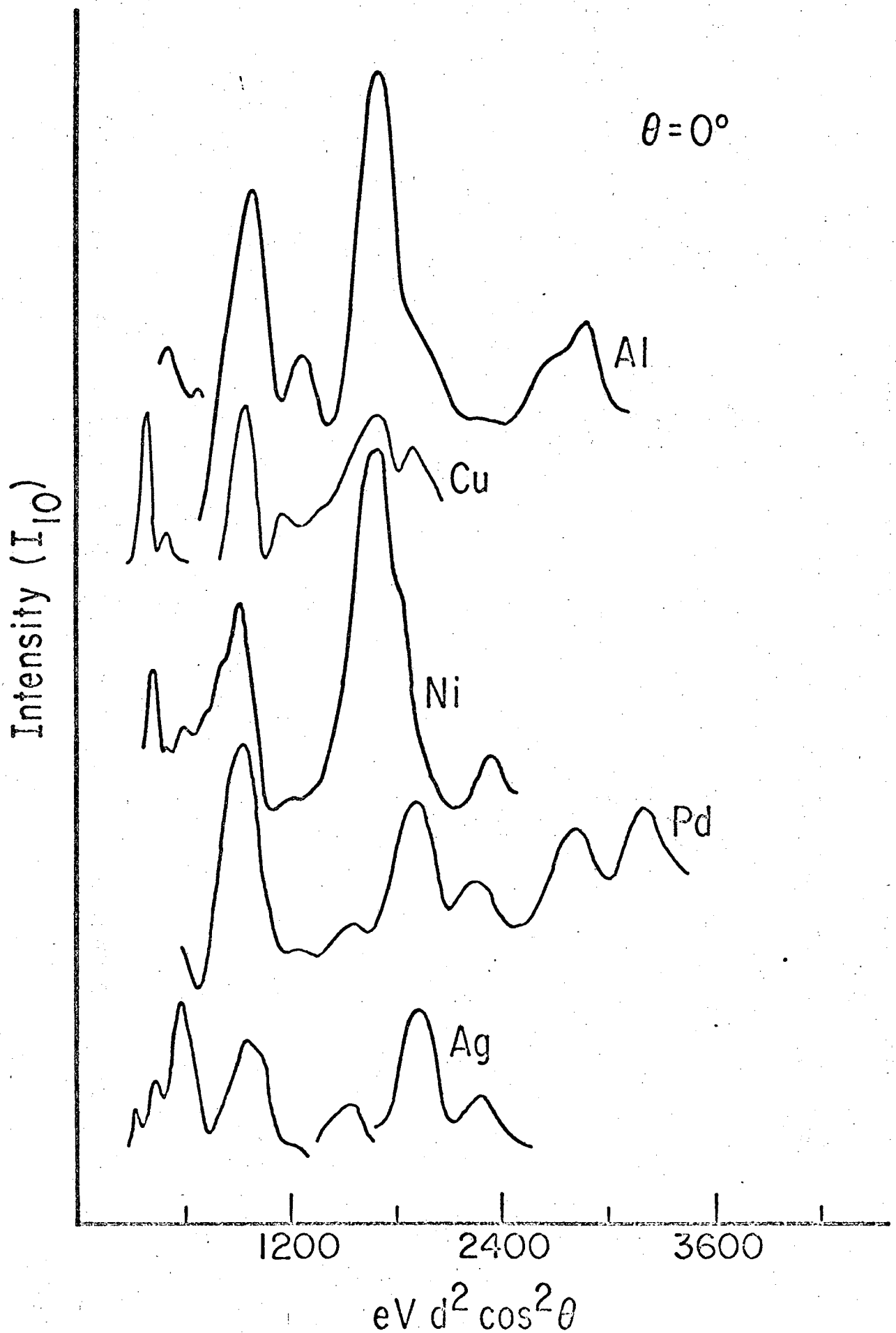

Figure 4a.

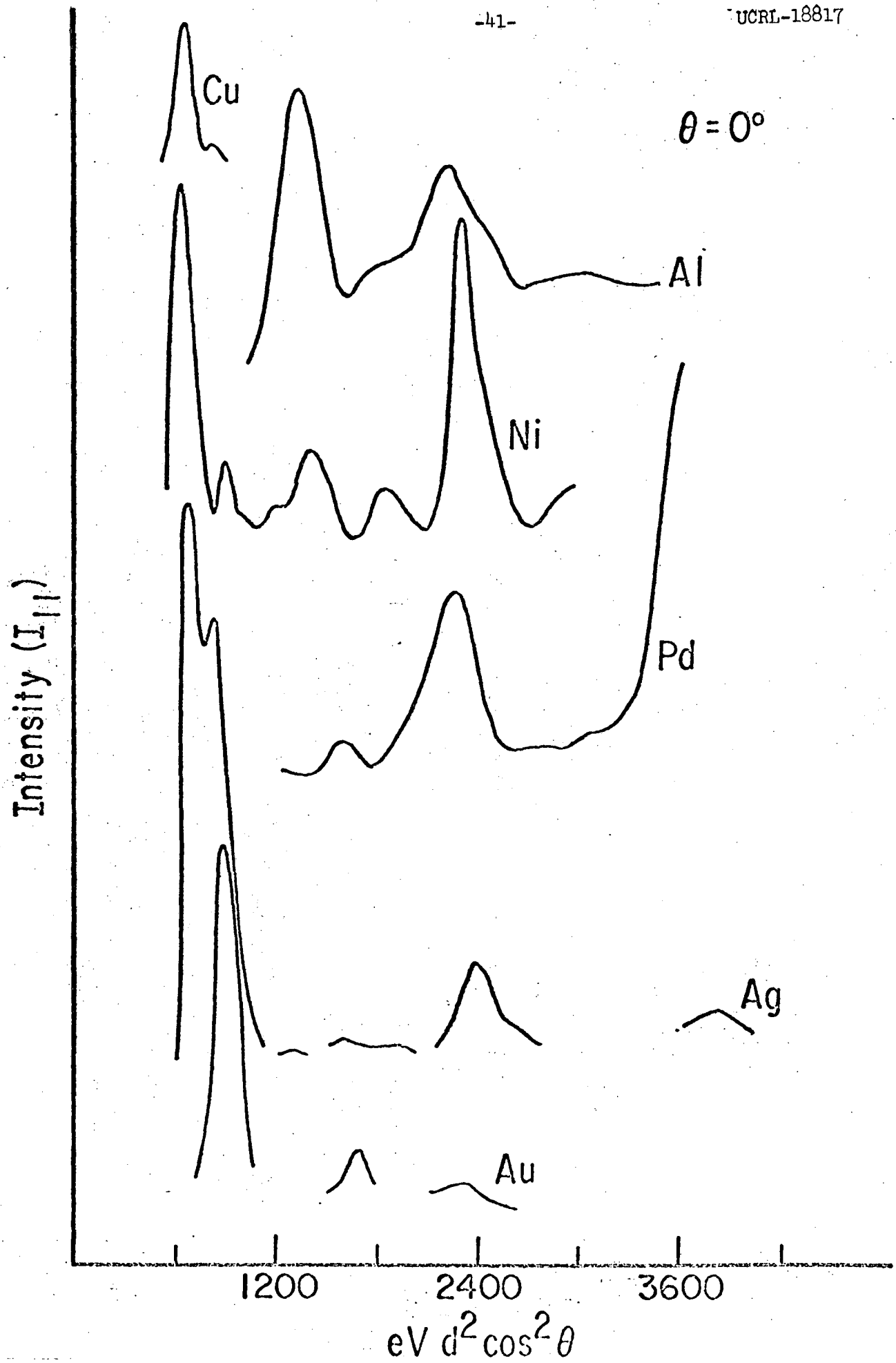

Figure 4b.

LEGAL NOTICE

This report was prepared as an account of Government sponsored work. Neither the United States, nor the Commission, nor any person acting on behalf of the Commission:

A. Makes any warranty or representation, expressed or implied, with respect to the accuracy, completeness, or usefulness of the information contained in this report, or that the use of any information, apparatus, method, or process disclosed in this report may not infringe privately owned rights; or

B. Assumes any liabilities with respect to the use of, or for damages resulting from the use of any information, apparatus, method, or process disclosed in this report.

As used in the above, "person acting on behalf of the Commission" includes any employee or contractor of the Commission, or employee of such contractor, to the extent that such employee or contractor of the Commission, or employee of such contractor prepares, disseminates, or provides access to, any information pursuant to his employment or contract with the Commission, or his employment with such contractor.

TECHNICAL INFORMATION DIVISION
LAWRENCE RADIATION LABORATORY
UNIVERSITY OF CALIFORNIA
BERKELEY, CALIFORNIA 94720